ELSEVIER

Journal of Alloys and Compounds 228 (1995) 54–58

Journal of ALLOYS AND COMPOUNDS

Magnetic phase transitions and magnetoresistance in easy-plane antiferromagnets $HoGa_2$ and $DyGa_2$

P.E. Markin, N.V. Baranov

Institute of Physics and Applied Mathematics, Ural State University, 620083 Ekaterinburg, Russian Federation

Received 7 March 1995

Abstract

The results of the magnetization and magnetoresistance studies performed on single crystals of hexagonal $HoGa_2$ and $DyGa_2$ compounds are presented. They have an antiferromagnetic alignment of the magnetic moments of R-ions in the basal plane below the Néel temperatures 7.6 and 11 K respectively. The field-induced multi-step magnetic phase transitions in the basal plane are accompanied by the great changes in the electrical resistivity of both compounds. Using data on the magnetoresistance, two field-induced intermediate phases in $HoGa_2$ are found, when the field was applied along the *a* axis, which is of easy magnetization. The magnetic phase diagram of $HoGa_2$ along *a* axes is determined.

Keywords: Rare-earth compounds; Field-induced magnetic phase transitions; Magnetoresistance

1. Introduction

The RGa_2 compounds are suitable objects for the investigation of magnetic properties and magnetic phase transitions in rare-earth intermetallics. These compounds crystallize in the hexagonal AlB_2-type structure with one rare-earth ion per crystallographic unit cell [1]. This crystal structure consists of layers of R and Ga atoms. At low temperatures the RGa_2 compounds have mainly a complex antiferromagnetic (AF) order [2]. Below the Néel temperatures, most of the compounds exhibit phase transitions from one antiferromagnetic configuration to another. The magnetic structures of RGa_2 result from the long-range RKKY interaction and crystal field effects.

Preliminary studies of $HoGa_2$ performed on polycrystalline samples by means of a.c. susceptibility and electrical resistivity, and also measurements of the magnetization on single crystals at 4.2 K, show that this compound has the antiferromagnetic order below $T_N = 7.6$ K, *a* ([100]) is the easy axis and *c* ([001]) is the hard axis [2,3]. The magnetization along the *a* axis reaches a value about 8.8 μ_B per Ho ion at a field of 8 T. According to neutron diffraction at 4.2 K [4], $HoGa_2$ has a colinear magnetic structure with Ho magnetic moments parallel to the *a* axis and with the propagation vector [0,1/2,0].

In $DyGa_2$ three antiferromagnetic phases below $T_N = 11$ K were observed. Measurements of magnetization on single crystals have shown that $DyGa_2$ exhibits many field-induced phase transitions both in the basal plane and along the *c* axis [5]. In a field of 7.5 T applied along the easy *b* [210] axis, the magnetic moment per Dy ion, μ_{Dy}, reaches a value about 9.6 μ_B, which is very close to the value for a free Dy^{3+} ion (10 μ_B). This indicates that the applying of such field destroys the antiferromagnetic structure of $DyGa_2$ and leads to the ferromagnetic alignment of the Dy magnetic moments.

Measurements of the electrical resistivity, magnetoresistance, thermoelectric power and Hall effect [6,7] in RGa_2 compounds show that the transport properties are very sensitive to the changes of the magnetic structure and can be used for detecting the magnetic phase transition in these compounds.

In this paper the results of magnetoresistance studies at field-induced magnetic phase transitions in $HoGa_2$ and $DyGa_2$ single crystals are presented.

2. Experimental details

$HoGa_2$ and $DyGa_2$ alloys were melted in He atmosphere in an arc furnace from components with purity

Elsevier Science S.A.
SSDI 0925-8388(95)01651-1

99.9% for Ho and Dy, and 99.99% for Ga. All the alloys were annealed at 800“ ”°C for three days. X-Ray diffraction of the powders was carried out using Cr Kα radiation. The amount of foreign phases for all the alloys was less than 5%. Single crystals were prepared in a resistance furnace by a modified Bridgman technique.

The magnetization measurements were made by a vibrating-sample magnetometer in fields up to 7 T in the temperature range from 2.2 K up to 300 K on single crystals of about $1.5 \times 1.5 \times 1.5$ mm^3 in size. The magnetoresistance was measured on $1 \times 1 \times 4$ mm^3 samples using a four-contact circuit in the temperature interval 1.9–10 K.

3. Results and discussion

Fig. 1 shows the temperature dependences of the reciprocal magnetic susceptibility measured in the paramagnetic region along and perpendicular to the c ([001]) axis of the $HoGa_2$ single crystals. Curie–Weiss behavior is observed above 100 K, with paramagnetic Curie temperatures of $\Theta_p^{\perp} = 1$ K and $\Theta_p^{\parallel} = -17$ K, and with an effective magnetic moment $\mu_{eff} = 10.6\ \mu_B$ per Ho ion. For the $DyGa_2$ single crystal we have obtained the values of the paramagnetic Curie temperatures, which are in good agreement with those presented in Ref. [5].

As is mentioned above, the magnetic properties of RGa_2 are mainly determined by the exchange interactions and magnetocrystalline anisotropy due to the crystal electric field (CEF). As is known, the second-order parameter B_2^0 of the crystal field hamiltonian can be obtained directly from the difference between two paramagnetic Curie temperatures $\Theta_p^{\perp}$ and $\Theta_{pp}^{\parallel}$. Using relations presented in Ref. [8] we have obtained $B_2^0 = 0.21$ K for $HoGa_2$.

Magnetization and magnetoresistance curves measured at $T = 2.2$ K on single crystals of $HoGa_2$ are presented in Fig. 2. As can be seen from Fig. 2(a), in low magnetic fields ($B < 1.7$ T) the anisotropy of the magnetization in the basal plane is absent and the magnetization process can be associated with the spin-flopping and with the rotation of Ho magnetic moments. The picture of the magnetization process in low fields is complicated by the presence of three equivalent easy axes in the basal plane. In higher magnetic fields ($B > 1.7$ T) the anisotropy in the basal plane appears. The field applied along the a axis gives rise to the anomaly on the magnetization curve in the field

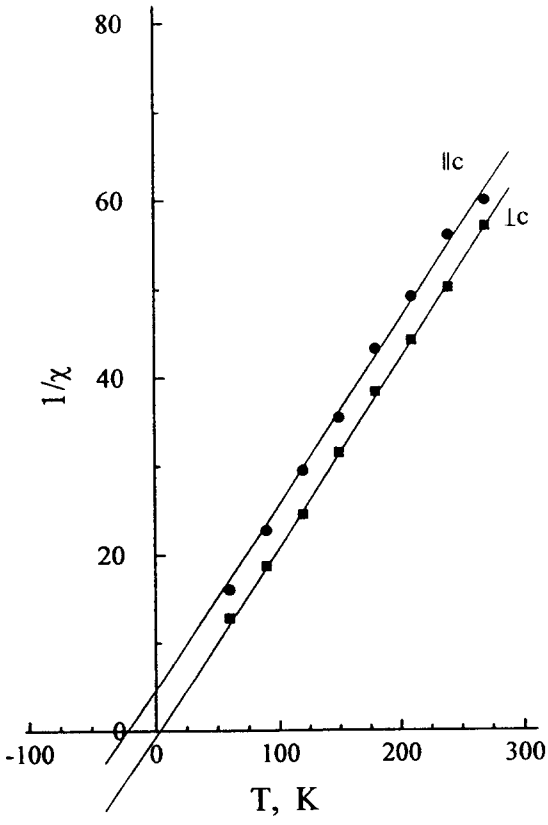

Fig. 1. Temperature dependences of the reciprocal susceptibility along the c axis and in the basal plane of a $HoGa_2$ single crystal.

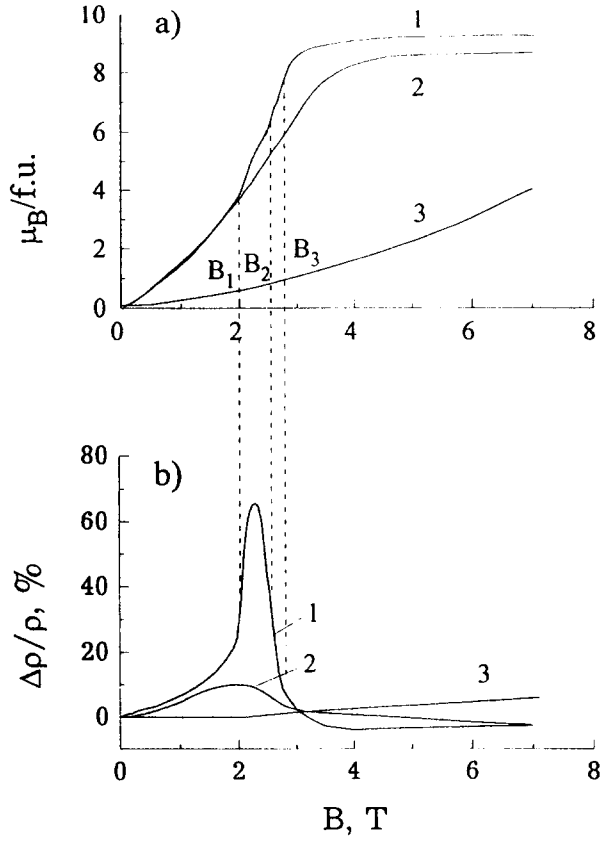

Fig. 2. (a) Magnetization and (b) longitudinal magnetoresistance vs. magnetic field for $HoGa_2$ at $T = 2.2$ K: curve 1, $B \| a$; curve 2, $B \| b$; curve 3, $B \| c$.

interval from 2 up to 2.6 T. This anomaly is absent when the field is applied along the b axis.

The anisotropy between the two axes in the basal plane of $HoGa_2$ can be also evidenced by the smaller high-field saturation value of μ_{Ho} along the b axis, $\Delta\mu = \mu_{Ho}(B\|a) - \mu_{Ho}(B\|b) \approx 0.6\ \mu_B$ in 7 T. These data are in agreement with earlier measurements of the magnetization at 4.2 K presented in Ref. [2], where the value of $\Delta\mu$ was found to be about 0.4 μ_B. It is necessary to note that at 4.2 K no visible anomalies on the magnetization curve along the a axis are observed. The magnetic anisotropy observed in the basal plane of $HoGa_2$ can be associated with sixth-order CEF parameter B_6^6 and can also be influenced by magnetoelastic effects. Unfortunately, the value of B_6^6 could not be obtained from our measurements.

The step of magnetization observed on the $\mu_{Ho}(B)$ curve along the a axis can indicate the appearance of an intermediate magnetic phase (I_1) in the field interval from B_1 up to B_2. In the fields from B_2 up to B_3 the phase transition from I_1 to the field-induced ferromagnetic (FM) state takes place (see Fig. 2(a)).

As follows from Fig. 2(b), the anisotropy of the magnetization in $HoGa_2$ reveals itself in the anisotropy of the longitudinal magnetoresistance, $\Delta\rho/\rho = [\rho(B) - \rho(0)]/\rho(0)$. The electrical resistivity increases gradually with the increasing field along the c axis where the Ho magnetic moments rotate gradually in the field direction. When the field is applied along the easy a axis, the giant peak of the magnetoresistance ($\Delta\rho/\rho$ up to 70%) is observed in the same field interval (B_1–B_2) where the step on the magnetization curve takes place. At the phase transition to the FM state at $B > B_2$ the electrical resistivity becomes lower than in the initial AF state at $B = 0$.

The change in the electrical resistivity of metallic antiferromagnets in the regions of phase transitions can be connected with several origins. An additional contribution to the electrical resistivity can result from the enhanced electron–magnon interaction near the critical field of the spin-flop transition [9]. Another reason for the increase of the electrical resistivity near the phase transition is the s-electron reflection from the potential barrier at the interphase boundary separating the phases with different magnetic structures [10,11]. The peaks of the magnetoresistance caused by this reflection were observed in the isostructural compound $ErGa_2$ in the intermediate state where the different magnetic phases coexist. The s-electron scattering on the magnetic moments distributed in the interphase boundaries, i.e. on the magnetic inhomogeneity, can also increase the electrical resistivity of the compound in the intermediate state. Moreover, the change of ρ in metallic antiferromagnets at the phase transitions may be produced by the deformation of the Fermi surface due to the appearance or disappearance of Brillouin superzones [12]. These superzones and the energy gaps on superzone boundaries result from the magnetic structure, with the unit cell having a larger period than the unit cell of the crystal lattice.

We have performed a detailed study of the longitudinal magnetoresistance of $HoGa_2$ single crystals when the field was applied along the a axis. Results of this study are presented in Figs. 3 and 4. From the field dependences of $\Delta\rho/\rho$ measured at various temperatures, we can distinguish two temperature intervals with different behavior of the magnetoresistance. Below the Néel temperature a flat and broad maximum of $\Delta\rho/\rho$ appears, and it becomes narrower with decreasing temperature down to $T \approx 3.6$ K, where this maximum vanishes. No peculiarities were observed in the magnetization curves at these temperatures. In the second temperature interval a new peak of $\Delta\rho/\rho$ appears at $T \approx 4.0$ K, and broadens with decreasing temperature.

Since the peak of magnetoresistance and the step on the $\mu_{Ho}(B)$ curve are observed in the same field interval (see Figs. 2(a), 2(b)), one can suggest that the features on the $\Delta\rho/\rho$ curves are associated with the presence of field-induced intermediate magnetic phases: I_1 at $T < 4.0$ K and I_2 in the temperature interval 3.6–7.6 K.

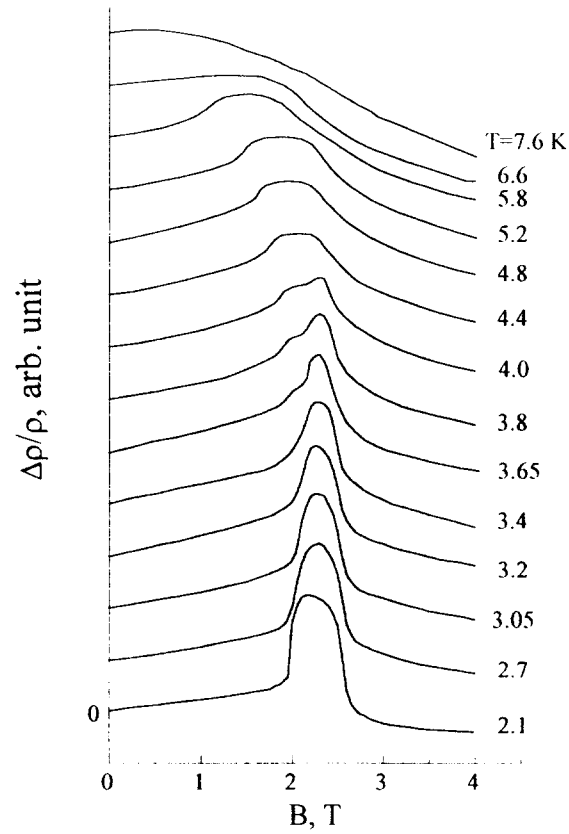

Fig. 3. Magnetoresistance curves measured at various temperatures along the a axis of $HoGa_2$.

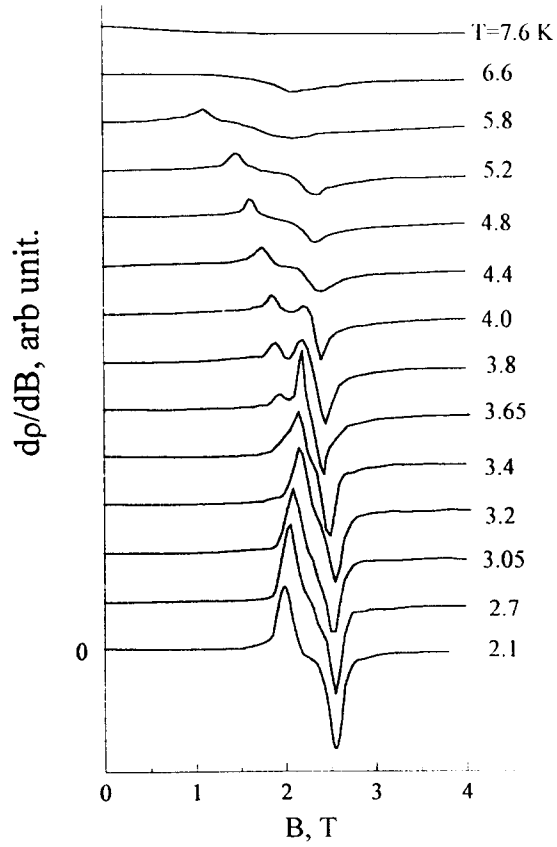

Fig. 4. $d\rho/dB$ vs. B obtained from the magnetoresistance curves presented in Fig. 3.

The peaks of $\Delta\rho/\rho$ in $HoGa_2$ cannot be the result of the enhanced electron–magnon interaction because the height of these peaks, as follows from Fig. 3, becomes higher with decreasing temperature, in contradiction to the theory of electron–magnon interaction [9]. The behavior of the magnetoresistance cannot also be connected with the presence of the interphase boundaries in the region of phase transitions because in this case two peaks of $\Delta\rho/\rho$ should be observed, the first peak before and the second peak after the step on the magnetization curve, as (for example) in $ErGa_2$ [10].

In our opinion the main reason for the peculiarities of the magnetoresistance in $HoGa_2$ is the deformation of the Fermi surface at the field-induced magnetic phase transitions owing to the appearance or disappearance of superzones and the energy gaps on superzone boundaries [12]. Indeed, the translation magnetic symmetry of the intermediate phases can be different from those of the initial antiferromagnetic state and of the field-induced ferromagnetic state. Deformations of the Fermi surface at the field-induced phase transition were observed in the isostructural $SmGa_2$ compound by means of measurements of the De Haas–Van Alphen effect [13]. In this compound, the step-like behavior of the magnetization and transverse magnetoresistance was found in the field applied along the c axis [7].

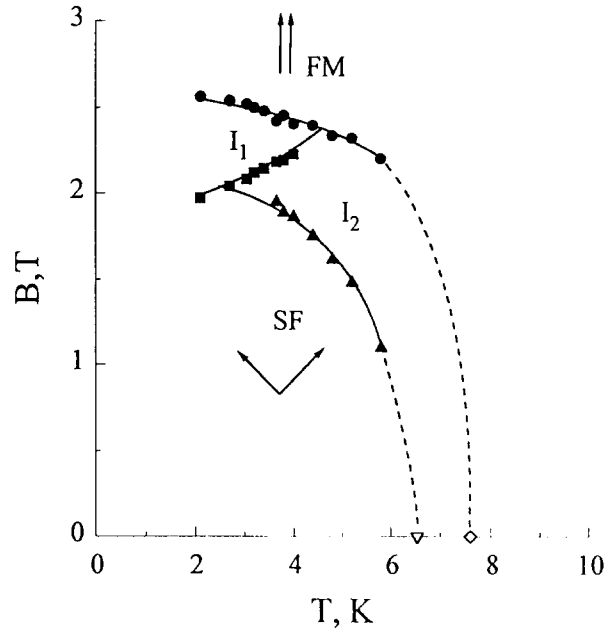

Fig. 5. Magnetic B–T phase diagram of $HoGa_2$ for $B\|a$: SF, spin-flop phase; FM, field-induced ferromagnetic phase; I_1, I_2, field-induced intermediate phases.

Fig. 4 shows the field dependences of the derivatives $d\rho/dB$ obtained numerically from the $\Delta\rho(B)/\rho$ curves presented in Fig. 3. The extreme values of $d\rho/dB$ indicate the critical fields of phase transitions along the a axis of $HoGa_2$. These data allow us to obtain the B–T phase diagram which is presented in Fig. 5. Neutron diffraction studies of magnetic structures in different magnetic fields are needed for the confirmation of this phase diagram.

Fig. 6 shows the field dependences of the magnetization and longitudinal magnetoresistance measured at 2.2 K along the a and b axes of $DyGa_2$ single crystals. The magnetization curves have a multi-step character and are in good agreement with the measurements presented in Ref. [5]. The field-induced phase transitions are accompanied by changes of electrical resistivity as in $HoGa_2$. As shown in Ref. [5], $DyGa_2$ has a complex magnetic phase diagram along three main axes. Measurements of the magnetoresistance at various temperatures can give more detailed information owing to the very high sensitivity to changes of the magnetic structure.

Acknowledgments

We are indebted to S.V. Zemlyanski for experimental support and to Professor E.V. Sinitsyn for helpful discussion.

This work was partly supported by a grant from the

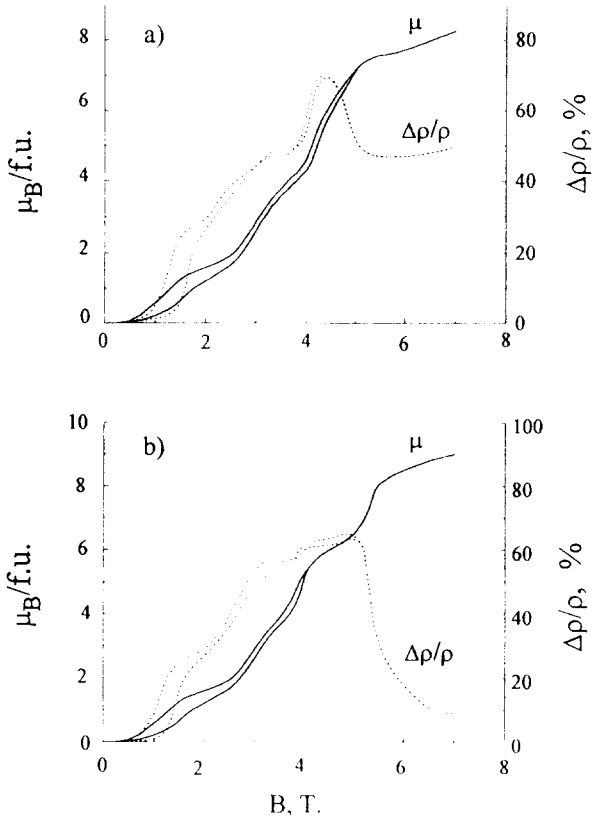

Fig. 6. Field dependences of (a) magnetization and (b) magnetoresistance for $DyGa_2$ at $T = 2.2$ K: curve 1, $B \| a$; curve 2, $B \| b$.

Higher Education Committee of the Russian Federation and by the Russian Foundation of Fundamental Research (Grant No.93-02-14197).

References

[1] A. Raman, *Z. Metallkd., 58* (1967) 179.
[2] T.H. Tsai, J.A. Gerber, K.W. Weymouth and D.J. Sellmyer, *J. Appl. Phys., 49* (1978) 1507.
[3] T.H. Tsai and D.J. Sellmyer, *Phys. Rev. B, 20* (1979) 4577.
[4] H. Asmat and D.Gignoux, *Inst. Phys. Conf. Ser., 37* (1978) 286.
[5] D. Gignoux, D. Schmitt, A. Taceuchi and F.U. Zhang, *J. Magn. Magn. Mater., 97* (1991) 15.
[6] J.A. Blanco, D. Gignoux, J.C. Gomez Sal, J. Rodriguez Fernandez and D. Schmitt, *J. Magn. Magn. Mater., 104–107* (1992) 1285.
[7] H. Henmi, Y. Aoki, T. Fukuharu, I. Sakamoto and H. Sato, *Physica B, 186–188* (1993) 655.
[8] A.A. Kazakov, *Fiz. Met. Metalloved., 28* (1969) 961 (in Russian).
[9] H. Yamada and S. Takada, *Progr. Theor. Phys, 49* (1973) 1401.
[10] N.V. Baranov, A.V. Deryagin, P.E. Markin and E.V. Sinitsyn, *Fiz. Nizk. Temp., 10* (1984) 781 (in Russian).
[11] N.V. Baranov, P.E. Markin, A.I. Kozlov and E.V. Sinitsyn, *J. Alloys Comp., 200* (1993) 43.
[12] R.J. Elliott, F.A. Wedgwood, *Proc. Phys. Soc., 81* (1963) 846.
[13] I. Sakamoto, T. Miura, H. Sato, T. Miyamoto, I. Shiozaki, I. Oguro and S. Maruno, *J. Magn. Magn. Mater. 108* (1992) 125.